

SUPPORTING INFORMATION

Super-strong Carbon Nanotube Fibers Achieved by Engineering Gas Flow and Post-Synthesis Treatment

Eugene Oh^{1‡}, Hyunjung Cho^{1‡}, Juhan Kim¹, Ji Eun Kim¹, Youngjin Yi¹, Junwon Choi¹, Haemin Lee², Ye Hoon Im¹, Kun-Hong Lee², and Won Jae Lee^{1*}*

¹ LG Chem R&D Campus Daejeon, 188 Munji-ro, Yuseong-gu, Daejeon, 34122, Republic of Korea

² Department of Chemical Engineering, Pohang University of Science & Technology, 77 Cheongam-Ro, Nam-Gu, Pohang, Gyeongbuk 37673, Republic of Korea

*Eugene Oh

E-mail: eugeneoh@lgchem.com

*Won Jae Lee

E-mail: iwjlee@lgchem.com

Contents

- S1. Raman, TEM, and SEM analysis of CNTFs for each case**
- S2. Photographs of catalyst clouds for cases 1 and 3**
- S3. Optimization of specific strengths of CNTFs using response surface methodologies**
- S4. Effects of reaction temperature on the specific strengths of CNTFs**
- S5. Effects of stretching rate on the specific strengths of CNTFs**
- S6. Wet-stretching process.**
- S7. Two-dimensional Fast Fourier Transform of SEM images**

S1. Raman, TEM, and SEM analysis of CNTFs for each case

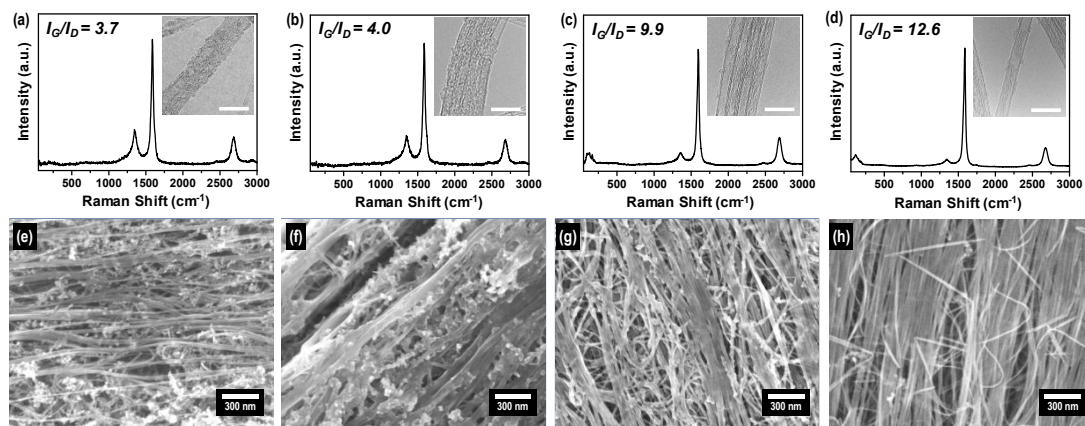


Figure S1. Raman spectra of CNTFs for (a) case 1, (b) case 2, (c) case 3, and (d) optimum conditions with the corresponding TEM images displayed as insets. The scale bars in the insets of (a)–(d) are 10 nm. SEM images of CNTFs for (e) case 1, (f) case 2, (g) case 3, and (h) optimum conditions.

S2. Photographs of catalyst clouds for cases 1 and 3

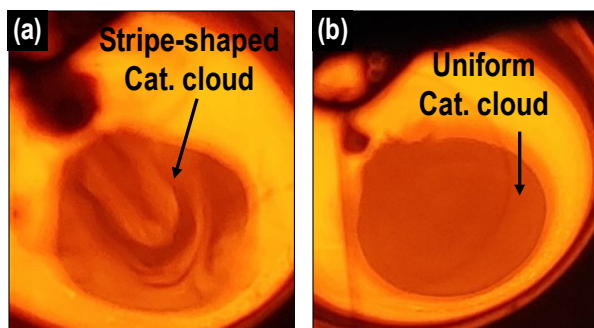


Figure S2. Photographs of catalyst clouds formed at the top of the reactor. (a) A stripe-shaped catalyst cloud in the formation of rotational flow for case 1 and (b) a uniform catalyst cloud in the absence of rotational flow for case 3.

S3. Optimization of the specific strengths of CNTFs using response surface methodologies

Response surface methodologies (RSM) were conducted to identify the optimal conditions for synthesizing high specific strength (SS) CNTFs. The RSM were designed using the Box–Behnken method suitable for CNTF fabrication experiments. The experimental variables were set as the input rates of ferrocene, thiophene, methane, and hydrogen, and the control range of each variable was set as shown in Table S1. A total of 27 experiments were sequentially performed (Table S2).

Table S1. Levels of the independent factors used in the 1st RSM.

Factors	Level		
	−1	0	1
Methane [sccm]	90	95	100
Ferrocene [mg/h]	19.7	27.5	35.4
Thiophene [mg/h]	140	170	200
Hydrogen [sccm]	1300	1400	1500

Table S2. Experimental conditions and results of the 1st RSM

No.	Coded levels of factors				Results
	Methane	Ferrocene	Thiophene	Hydrogen	<i>SS</i> [N/tex]
1	−1	−1	0	−1	1.58
2	0	0	−1	−1	2.08
3	1	0	1	−1	1.46
4	0	1	0	−1	1.46
5	−1	0	−1	−1	1.26
6	−1	0	1	−1	1.24
7	1	0	−1	−1	1.92
8	0	1	−1	−1	0.93
9	0	−1	0	−1	1.3
10	−1	1	0	−1	0.84
11	−1	0	0	−1	0.82
12	1	1	0	−1	1.35

13	0	1	1	-1	1.05
14	-1	0	0	-1	1.37
15	1	0	0	-1	1.08
16	0	1	0	-1	0.88
17	0	-1	0	-1	1.51
18	1	-1	0	-1	1.74
19	0	0	1	-1	1.51
20	0	0	0	-1	1.51
21	0	-1	-1	-1	1.46
22	1	0	0	-1	1.5
23	0	-1	1	-1	1.6
24	0	0	1	-1	1.09
25	0	0	-1	-1	1.04
26	0	0	0	-1	1.28
27	0	0	0	-1	1.28

A mixture of H₂ (1.3 slpm) and N₂ (0.6 slpm) was used as the carrier gas. The maximum reaction temperature was set to 1220°C. A CNT sock formed and reached the bottom of the reactor approximately 1 min after the precursors were input. The sock passed through the water and was converted to CNTFs. The winding rate of the CNTFs was 4.5 m/min.

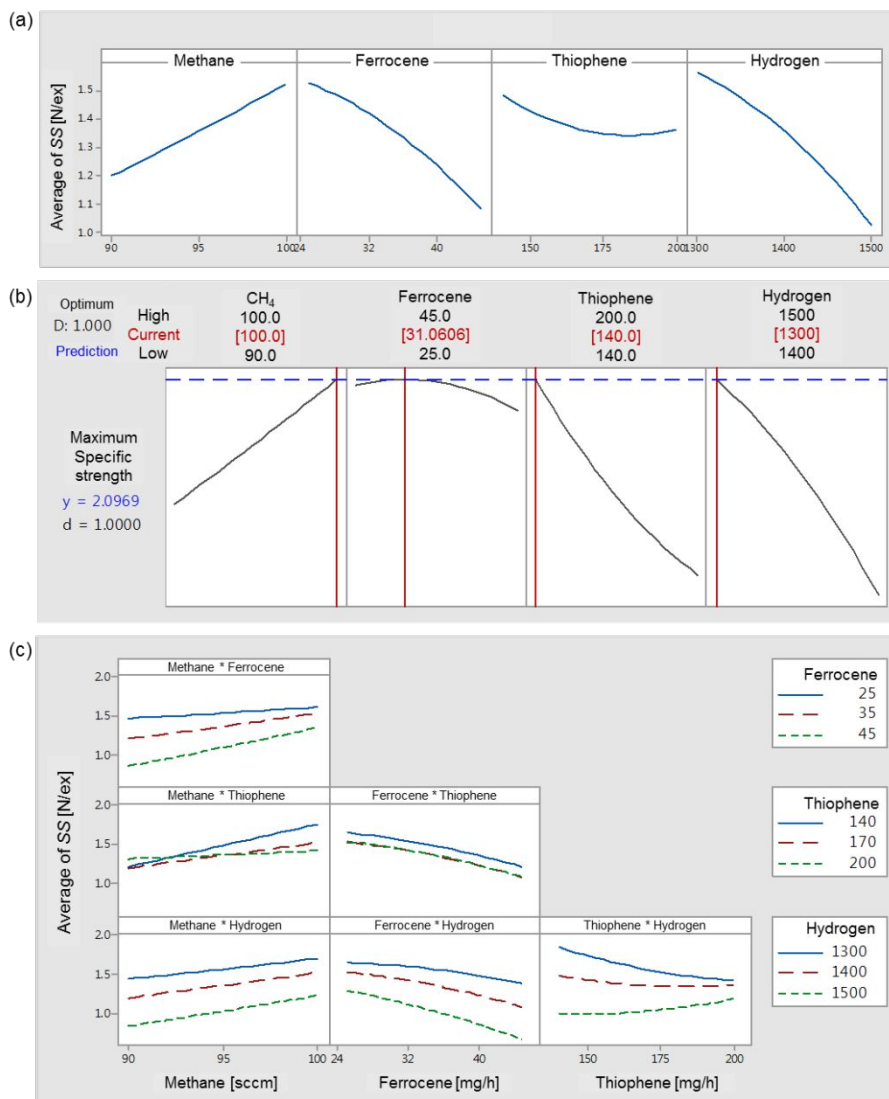


Figure S3. Results of the 1st RSM to the SS: (a) plots of the main effects, (b) reaction optimization, and (c) interaction effect plots. The SS of the CNTFs was determined to be most affected by the methane, ferrocene, and hydrogen inputs.

For the main effects of RSM results (Fig. S3(a)), the SS of the CNTFs was determined to be most affected by the methane, ferrocene, and hydrogen inputs. To maximize the SS, the input rates of hydrogen and ferrocene should be decreased and the methane input rate should be increased, i.e., it is advantageous to improve the SS of the CNTFs by synthesizing under conditions that the amount of catalyst is low and the carbon-to-hydrogen ratio is high (Fig. S3(b)). Finally, no interaction effects were observed between the variables because the p-value, which discriminates the interactions, was less than 0.05 (Fig. S3(c)).

To determine a more accurate optimal point for high SS, we moved the experimental window (Table S3) and proceeded to the 2nd RSM. In the 2nd RSM, the experimental conditions were modified to slightly reduce the input rates of ferrocene and methane while the input rates of hydrogen and thiophene (140 mg/h) were set as constant values. The experiments were conducted for a total of 15 different conditions (Table S4).

Table S3. Levels of the independent factors used in the 2nd RSM.

Factors	Level		
	−1	0	1

Hydrogen [L/min]	1.25	1.3	1.35
Ferrocene [mg/h]	15.7	23.6	31.5
Methane [sccm]	90	95	100

Table S4. Experimental conditions and results of the 2nd RSM

No.	Coded levels of factors			Results
	Hydrogen	Ferrocene	Methane	<i>SS</i> [N/tex]
1	0	1	−1	0.94
2	−1	1	0	1.43
3	1	−1	0	1.58
4	−1	0	1	1.36
5	1	0	−1	1.07
6	−1	0	−1	1.38
7	1	1	0	0.88
8	0	0	0	1.41

9	0	-1	1	1.91
10	0	0	0	1.59
11	1	0	1	1.57
12	-1	-1	0	2.20
13	0	1	1	1.73
14	0	-1	-1	1.68
15	0	0	0	1.51

In the main effect diagram, the 2nd RSM showed that the SS of the CNTFs was most influenced by the input rates of methane and ferrocene (Fig. S4(a)). To maximize the SS, the amount of ferrocene input should be decreased and the methane input amount should be increased. The optimum input rate of ferrocene was less than 15.7 mg/h, which is not included in the experimental window (Fig. S4(b)). To further increase the SS, the amount of catalyst precursor should be further reduced. However, because CNTFs cannot be produced continuously under the critical mass concentrations of the catalyst, the input rates of the catalyst precursor cannot be further reduced.¹ Finally, no interaction effects were observed between variables because the p-value, which discriminates the interaction, was less than 0.05 (Fig. S4(c)).

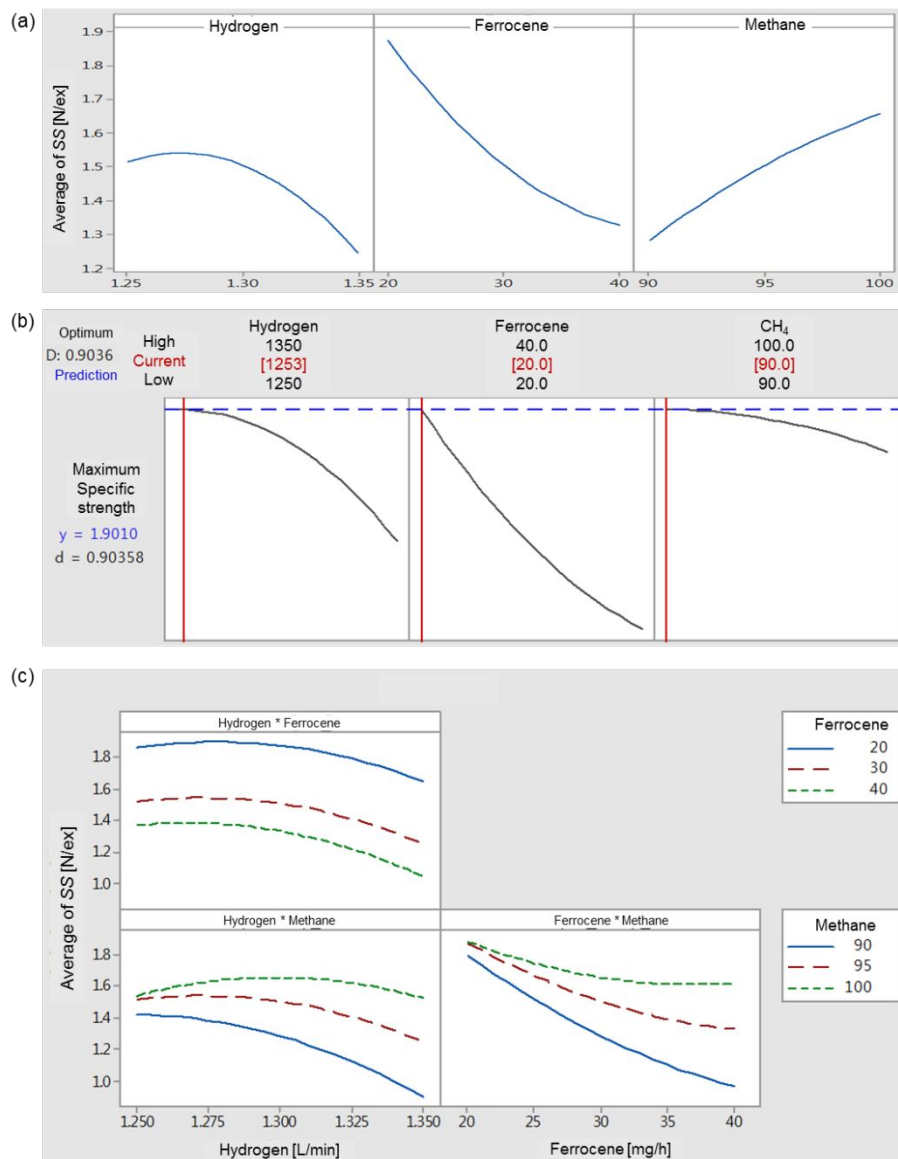


Figure S4. Results of the 2nd RSM on the SS: (a) plots of the main effects, (b) reaction optimization, and (c) plots of the interaction effect. The SS of the CNTFs was determined to be most affected by methane and ferrocene.

S4. Effects of reaction temperature on the specific strengths of CNTFs

In Fig. 1(a) of the main manuscript, the average SS increased from 0.4 N/tex to 1.2 N/tex at a reaction temperature of 1200°C owing to the decreased inner diameter and the modified tube material of the reactor. However, the RSM experiments, as shown in the Supporting Information section S3, were performed at 1220°C. Under the same experimental conditions, the SS of the CNTFs was higher at 1220°C than at 1200°C because the evaporation of catalyst particles was more active at 1220°C. The recrystallization rates of the catalyst particles may be affected by the reaction temperature. Above the melting point of the FeS catalyst particles (e.g., 1194°C), these particles were completely evaporated and then re-nucleated, thus resulting in the small diameters of the catalyst particles when the CNTs were synthesized.² Therefore, because of the small diameters of the CNTs synthesized at 1200°C, the cohesive force of the formed CNT sock increased and bundles of larger sizes formed.

Conversely, the SS of the CNTFs decreased at temperatures greater than 1220°C (e.g., 1250°C) because the zone in which CNT synthesis is possible is shorter at higher reaction temperatures owing to the constant reactor length.²

S5. The effects of the stretching ratio on the specific strengths of the CNTFs

The SS of the CNTFs gradually increased as the stretching ratio increased for a range of ratios from 0% to 12%.

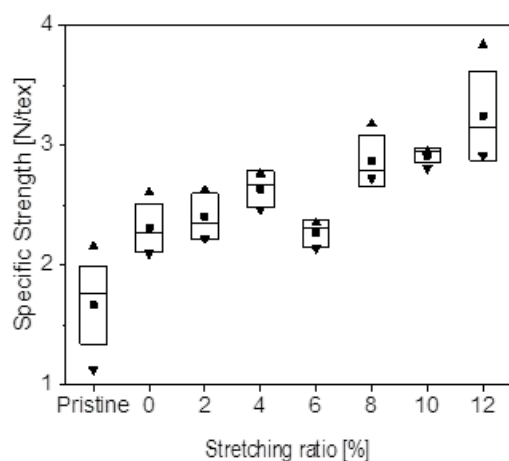


Figure S5. Graph indicating the relationship between the stretching ratios of the CNTFs and their SS for a range of low stretching ratios.

S6. Wet-stretching process

Because chlorosulfonic acid (CSA) is a superacid and reacts violently with moisture in the air to release gaseous hydrochloric acid, the wet-stretching process using CSA should be conducted under conditions of extremely low humidity. Therefore, we used a glove box made of LDPE (portable glove box, Bel-Art products, US) and acid-resistant gloves (F-Telon glove B-22L, As One, Japan), as shown in Fig. S6(a).

Moreover, wet-stretching of the CNTFs was performed in the LDPE glove box. The CNTFs were attached to the two TPFE parts of the custom-made stretching equipment using adhesive tape as shown in Fig. S6(b, c). The CNTFs were fixed on the equipment and immersed in the CSA for 5 min and were then stretched. After wet-stretching, the CNTFs were washed with acetone and then subjected to heat treatment at 300°C for 30 min in an air atmosphere.

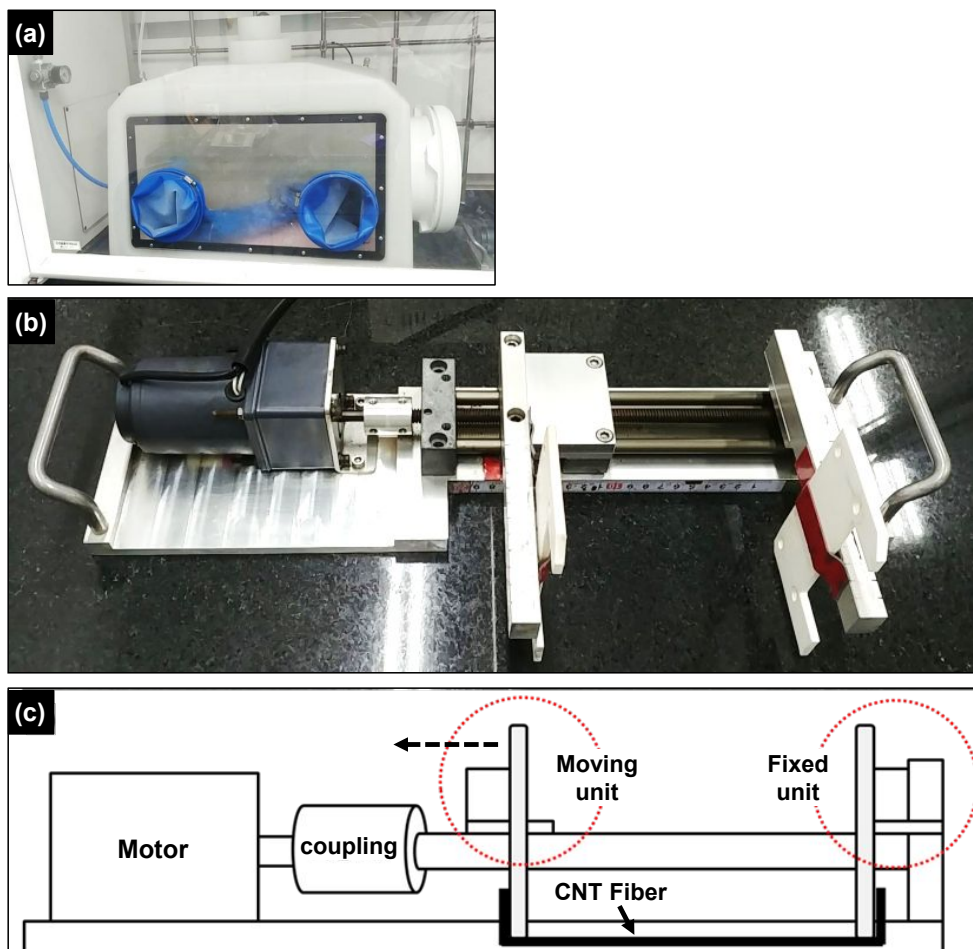


Figure S6. Photo images of (a) PTFE glove box and (b) apparatus for CNTF stretching. (c) A drawing of the custom-made stretching equipment displayed in Fig. S6(b).

S7. Two-dimensional Fast Fourier Transform of SEM images

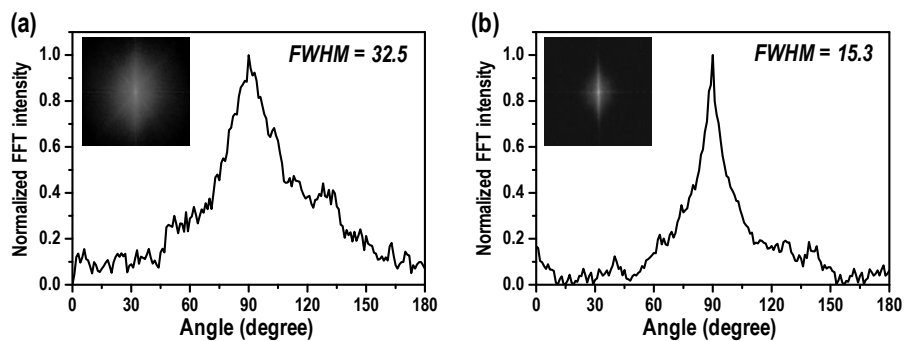


Figure S7. Radial-sum intensity profiles of (a) pristine and (b) 24% wet-stretched CNTFs from 0 to 180 degrees with the corresponding FFT patterns shown as insets.

References

1. Hoecker, C.; Smail, F.; Pick, M.; Weller, L.; Boies, A. M. The Dependence of CNT Aerogel Synthesis on Sulfur-driven Catalyst Nucleation Processes and a Critical Catalyst Particle Mass Concentration. *Sci. Rep.* **2017**, 7, 14519.
2. Hoecker, C.; Smail, F.; Pick, M.; Boies, A. M. The Influence of Carbon Source and Catalyst Nanoparticles on CVD Synthesis of CNT Aerogel. *Chem. Eng. J.* **2017**, 314, 388–395.